

1.11-Mev state would establish an $E2/M1$ mixing ratio and aid in interpreting the 0.37-1.11-Mev angular correlation. Angular correlation studies of the low intensity 0.95-0.77-, 0.85-0.77-, 0.61-1.11-, and 0.51-1.11-Mev cascades which have been reported³² in the decay of Ni^{65} would give additional data on transitions between various members of the excited quartet of states.

ACKNOWLEDGMENTS

The authors wish to thank Dr. D. E. Alburger for the use of and assistance with the beta spectrometer. We are indebted to Dr. A. Schwarzschild and Dr. J. Wenner for many helpful discussions. The continued cooperation of Dr. C. P. Baker and the cyclotron operating staff is gratefully acknowledged.

Coulomb Excitation of the Second $2+$ States in W, Os, and Pt Nuclei

F. K. MCGOWAN AND P. H. STELSON
Oak Ridge National Laboratory, Oak Ridge, Tennessee
(Received January 5, 1961)

The location of a second $2+$ state has been established for six even-even nuclei by means of Coulomb excitation produced by 4- to 5-Mev protons. The relatively weak excitation of these states is detected by a measurement of the gamma-ray yields from singles spectra and from coincident measurements of the cascade gamma rays. The $B(E2)$'s for decay of the second $2+$ state to ground state by the crossover transition exhibit some uniformity for the even-even isotopes of W and Os, being about 6 times the single-particle value. The cascade/crossover ratio for the decay of the second $2+$ state is known for these nuclei. The upper cascade $B(E2)$'s exhibit enhancements of 10 to 60 times the single-particle value. The ratios of the $B(E2)$'s for decay of the first and second $2+$ states are compared to the predictions of several collective models. For five of these nuclei the $E2/M1$ ratio is known for the upper cascade transition. The $B(M1)$ values obtained are exceedingly small compared to the single-particle estimate. This result is in qualitative agreement with the collective models which predict that $M1$ radiation is forbidden in the decay of vibrational excitations.

I. INTRODUCTION

THE level structures of the nuclei of the neighboring elements wolfram, osmium, and platinum suggest that these nuclei mark a rather gradual boundary for the rare-earth group of spheroidal nuclei. The even- A nuclei of wolfram exhibit the characteristic rotational bands of spheroidal nuclei. On the other hand, the platinum nuclei have no recognizable rotational bands, but have, instead, spectra somewhat suggestive of the near-harmonic spectra observed for many medium-weight nuclei. The spectra of the osmium nuclei are particularly interesting because these nuclei link the wolfram and platinum nuclei.

In addition to the rotational band based on the ground state, the even- A rare-earth nuclei systematically exhibit rotational bands based on excited states at approximately 1-Mev excitation.¹ These excited states have properties expected for β - and γ -vibrational states. In particular, it has proved possible to observe the weak Coulomb excitation of the high-lying second $2+$ γ -vibrational state in the even- A wolfram nuclei. Whereas the first $2+$ state is observed to continuously increase in energy as one moves out of the spheroidal

region, the second $2+$ state systematically decreases in energy as the platinum nuclei are approached. It is therefore possible to also measure the Coulomb excitation of this state for osmium and platinum nuclei.

We wish to report the excitation energies and $B(E2)$ values obtained from the Coulomb excitation of $2+$ states in W^{184} , W^{186} , Os^{188} , Os^{190} , Os^{192} , Pt^{194} , and Pt^{196} . Similar results have been obtained for nuclei in this region by Barloutaud *et al.*² and for W^{182} , W^{184} , and W^{186} by Alkhazov *et al.*³

In our experiments, the Coulomb excitation cross section for the second $2+$ state is deduced from the yield of the de-excitation γ rays. A virtue of this method is that, in addition to obtaining the $B(E2)$ for decay of the second $2+$ state directly to the ground state, one also obtains the $B(E2)$ for decay of the second $2+$ state to the first $2+$ state. In some cases the $M1$ - $E2$ mixture for the $2'+ \rightarrow 2+$ transition is known. Having both the $M1$ - $E2$ mixture and the $B(E2)$ for the $2'+ \rightarrow 2+$ transition, one can then obtain the value for $B(M1)$ for the $2'+ \rightarrow 2+$ transition.

² R. Barloutaud, A. Leveque, P. Lehmann, and J. Quidort, *J. phys. radium* **19**, 60 (1958).

³ D. G. Alkhazov, A. P. Grinberg, G. M. Gusinskii, K. I. Erokhina, and I. Kh. Lemberg, *J. Exptl. Theoret. Phys. (U.S.S.R.)* **35**, 1325 (1958) [translation: *Soviet Phys.—JETP* **8**, 926 (1959)].

¹ See, e.g., the review paper by R. K. Sheline, *Revs. Modern Phys.* **32**, 1 (1960).

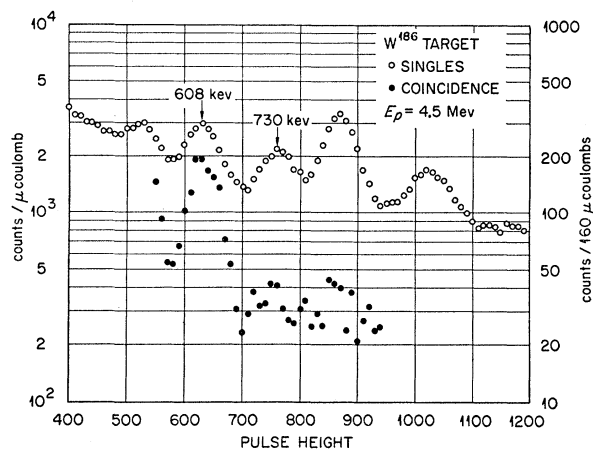


FIG. 1. Singles and coincident spectra of the gamma rays from Coulomb excitation of W^{186} .

Davydov and co-workers^{4,5} have developed in considerable detail possible types of collective motion which are directly applicable to a transitional region such as that of the osmium nuclei. Kane *et al.*⁶ have recently reported work on the level structure of Os^{190} . They find encouraging agreement between experiment and the prediction of Davydov and co-workers. We have carried out a comparison of our results with the predictions of the Davydov-Filippov model.

II. EXPERIMENTAL PROCEDURE

The projectiles used for effecting Coulomb excitation were variable-energy protons accelerated by the 5.5-Mv ORNL electrostatic generator. The target support arrangement and methods of measuring yields and angular distributions of gamma rays have already been described.^{7,8} For most of the coincident spectrum measurements the 3- \times 3-in. NaI(Tl) crystals were located 55° and 235° with respect to the incident ion beam with source to the detector distances of 4 and 5 cm, respectively. A fast-slow coincidence circuit was used with a resolving time $2\tau = 0.12 \mu\text{sec}$. Pulses from one of the detectors were fed into a single-channel analyzer whose window included the full energy peak of the gamma ray resulting from the decay of the first $2+$ state. The coincident spectrum from the other detector was displayed on a multichannel analyzer.

The platinum target, which contained 65.9% Pt^{196} , was prepared by sintering the metallic powder into a foil 120 mg/cm^2 in thickness. The tungsten targets,

which had been made previously to measure Coulomb excitation of the first $2+$ state, were prepared from enriched isotopes.⁹ The osmium target was prepared from the normal element by sintering the metallic powder into a foil. Enriched isotopes of osmium were not available for these measurements.

A. Gamma-Ray Spectra

The singles and coincident spectra for W^{186} are shown in Fig. 1. In contrast to the situation for the medium-weight elements, the excitation of the second $2+$ state is sufficiently strong to allow gamma-ray intensity measurements from the singles spectrum. Troublesome light elements impurities are present, however, in the enriched tungsten targets. For example, the sample of W^{186} contained by weight 600 ppm Si, 50 ppm Al, and 700 ppm Fe. These impurities produced the following troublesome gamma rays: Al(p, p') 0.842, 1.013, and 2.19 Mev; Al($^{27}p, \alpha\gamma$) 1.37 Mev; Si($^{28}p, p'$) 1.78 Mev, and Fe($^{56}p, p'$) 0.845 Mev. Similar impurities were observed in the enriched W^{184} target. As a result, the excitation of the second $2+$ state in W^{184} was obtained from measurements on a normal tungsten foil in which the light element impurity content was much less. The results for W^{186} and W^{184} are consistent with the

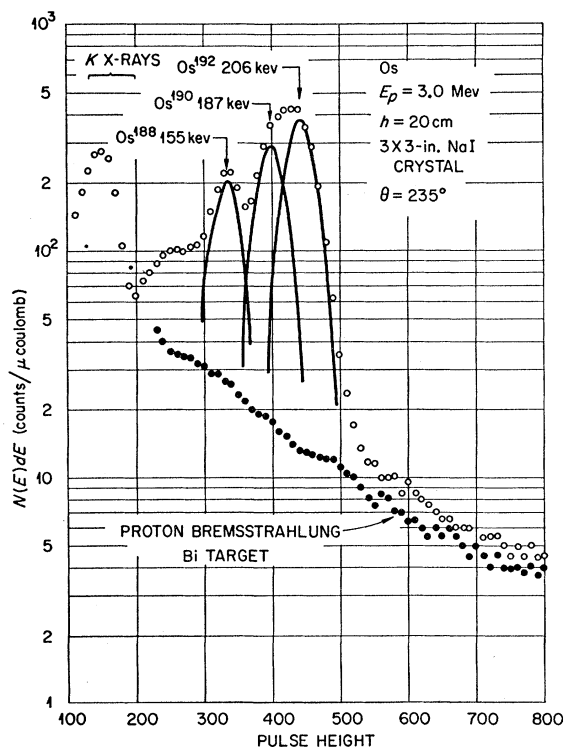


FIG. 2. Singles spectrum of the gamma rays from Coulomb excitation of the first $2+$ states in the even-even isotopes of osmium.

⁴ A. S. Davydov and G. F. Filippov, *Nuclear Physics* **8**, 237 (1958).

⁵ A. Davydov, *Proceedings of the International Conference on Nuclear Structure, Kingston, Canada, August 29–September 3, 1960*, edited by D. A. Bromley and E. W. Vogt (University of Toronto Press, Toronto, Canada, 1960), p. 801.

⁶ W. R. Kane, G. T. Emery, G. Scharff-Goldhaber, and M. McKeown, *Phys. Rev.* **119**, 1953 (1960).

⁷ P. H. Stelson and F. K. McGowan, *Phys. Rev.* **110**, 489 (1958).

⁸ F. K. McGowan and P. H. Stelson, *Phys. Rev.* **106**, 522 (1957).

⁹ The isotopically enriched samples were obtained from the Stable Isotopes Division of the Oak Ridge National Laboratory.

TABLE I. Reduced transition probabilities obtained from Coulomb excitation of the second $2+$ states in W, Os, and Pt. The number of excitations per μcoul for thick-target bombardment by protons is given on a 100% isotopic enrichment basis. The evaluation of the integral is given in units of keV mg/cm^2 .

Nucleus	Excitation (keV)	E_p (MeV)	Abundance (%)	Excitations per μcoul	Method	$\int_0^{E_i} \frac{g_2(\xi, \eta_i) E' dE}{dE/d\rho x} B(E2)_{\text{exo}} \times 10^{40}$ ($\text{cm}^2 e^2$)
W^{184}	891 ± 9	5.000	30.6	$(7.0 \pm 1.8) \times 10^4$	singles	2.60×10^4
		5.028	30.6	$(5.2 \pm 1.6) \times 10^4$	coincidence	2.72×10^4
W^{186}	730 ± 7	4.000	97.17	$(2.6 \pm 0.4) \times 10^4$	singles	9.54×10^3
		4.500	97.17	$(6.3 \pm 0.9) \times 10^4$	singles	2.45×10^4
		5.000	97.17	$(11.7 \pm 1.6) \times 10^4$	singles	5.07×10^4
		4.526	97.17	$(4.9 \pm 0.7) \times 10^4$	coincidence	2.56×10^4
		4.526	97.17	$(6.3 \pm 0.9) \times 10^4$	singles	2.56×10^4
		5.028	28.4	$(11.5 \pm 1.6) \times 10^4$	coincidence	5.26×10^4
		5.028	28.4	$(13.2 \pm 1.8) \times 10^4$	singles	5.26×10^4
						1.84
Os^{188}	633 ± 6	4.500	13.3	$(10.2 \pm 3.0) \times 10^4$	coincidence	3.64×10^4
		5.028	13.3	$(1.92 \pm 0.56) \times 10^5$	coincidence	7.24×10^4
Os^{190}	557 ± 6	4.500	26.4	$(1.20 \pm 0.24) \times 10^5$	coincidence	5.05×10^4
		5.028	26.4	$(2.04 \pm 0.41) \times 10^5$	coincidence	9.47×10^4
Os^{192}	489 ± 5	4.000	41.0	$(9.5 \pm 2.4) \times 10^4$	singles	3.42×10^4
		4.500	41.0	$(1.96 \pm 0.49) \times 10^5$	singles	6.78×10^4
		5.000	41.0	$(3.27 \pm 0.82) \times 10^5$	singles	1.17×10^5
		4.500	41.0	$(1.80 \pm 0.45) \times 10^5$	coincidence	6.78×10^4
		5.028	41.0	$(2.35 \pm 0.59) \times 10^5$	coincidence	1.20×10^5
						1.57
Pt^{196}	688	4.500	65.9	$< 3.3 \times 10^2$	coincidence	2.66×10^4
		5.028	65.9	$< 1.2 \times 10^3$	coincidence	5.65×10^4

Coulomb excitation of $2+$ states at (730 ± 7) keV and (891 ± 9) keV, respectively.

As mentioned above, separated isotopes of osmium were not available. However, the locations of the first $2+$ states of Os^{188} (155 keV), Os^{190} (187 keV), and Os^{192} (206 keV) are well known (see Fig. 2). Therefore, by coincident measurements it was possible to identify

and assign the corresponding second $2+$ states (see Fig. 3). Unfortunately, the osmium target contained appreciable impurities (150 ppm Al, 1000 ppm Si, and 700 ppm Fe) and the γ rays from these impurities made it difficult to obtain accurate intensity measurements of the Coulomb-excited osmium gamma rays in the singles spectra. The results from these measurements are summarized in Table I.

B. Angular Distributions

The angular distributions of the 730- and 608-keV gamma rays from W^{186} were measured for 5-MeV protons incident on a normal tungsten target. The results are consistent with the excitation of a $2+$ state at 730 keV in W^{186} . The distribution of the 608-keV gamma rays from the $2' \rightarrow 2$ transition is consistent with $(E2/M1)^{\frac{1}{2}} = -(30_{-10}^{+25})$ in the notation of Biedenharn and Rose.¹⁰

C. Extraction of $B(E2)_{\text{exo}}$

For most of the nuclei investigated, the gamma-ray yields were measured at several proton energies to determine whether the yield varied correctly for the Coulomb excitation process. We have assumed that the excitation of the second $2+$ state is due entirely to direct $E2$ excitation *via* the cross-over transition for the results given in Table I.

An alternative mode of excitation of the second $2+$ state by the "double $E2$ " mechanism is, in general, to

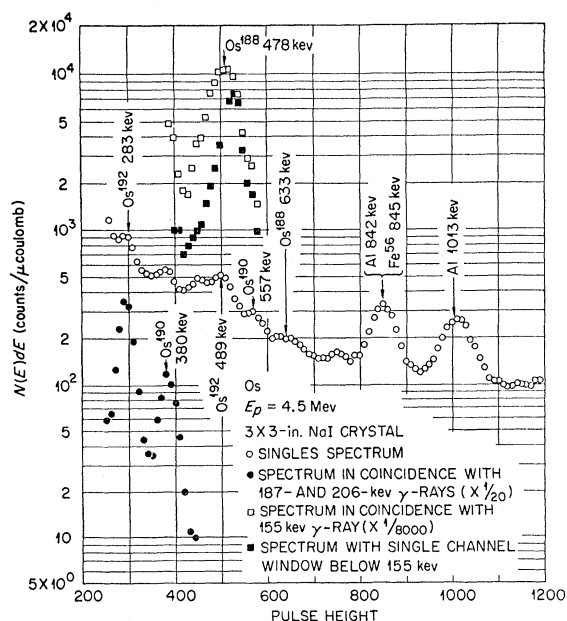


FIG. 3. Singles and coincident spectra of the gamma rays from Coulomb excitation of the second $2+$ states in the even-even isotopes of osmium.

¹⁰ L. C. Biedenharn and M. E. Rose, Revs. Modern Phys. **25**, 729 (1953).

TABLE II. Summary of quantities obtained from $B(E2)_{\text{exo}}$. The value of $B(E2)_d$ is given in column 5 for the downward transition listed in column 4. The ratio cascade/crossover is the ratio of total transitions by cascade to crossover.

Nucleus	E (kev)	$B(E2)_{\text{exo}}$ (cm ² e ²)	Transition	$B(E2)_d$ (cm ² e ²)	(Cascade crossover)	$(E2/M1)^{\frac{1}{2}}$	α_T	$B(M1)_d$	$\frac{B(E2)_d}{B(E2)_{\text{sp}}}$
⁷⁴ W ¹⁸⁴	111	(4.45 ± 0.45) × 10 ⁻⁴⁸	2 → 0	(8.9 ± 0.9) × 10 ⁻⁴⁹	1.0 ± 0.2 ^a	$(E2/M1) \geq 200^b$	2.66	$\leq 1.4 \times 10^{-4}$	143
	780 ± 8		2' → 2	(6.5 ± 1.9) × 10 ⁻⁵⁰			0.0075		10
	891 ± 9	(1.7 ± 0.5) × 10 ⁻⁴⁹	2' → 0	(3.4 ± 1.0) × 10 ⁻⁵⁰			0.0057		5.5
	122.5	(3.56 ± 0.37) × 10 ⁻⁴⁸	2 → 0	(7.13 ± 0.73) × 10 ⁻⁴⁹			1.83		113
W ¹⁸⁶	608 ± 6		2' → 2	(8.6 ± 1.5) × 10 ⁻⁵⁰	1.0 ± 0.2	$-(30-10^{+25})$	0.0133	$(2.5-1.7^{+3}) \times 10^{-5}$	13
	730 ± 7	(1.7 ± 0.3) × 10 ⁻⁴⁹	2' → 0	(3.5 ± 0.6) × 10 ⁻⁵⁰			0.0083		5.5
	155	(2.84 ± 0.31) × 10 ⁻⁴⁸	2 → 0	(5.69 ± 0.63) × 10 ⁻⁴⁹			0.851		89
	478 ± 5		2' → 2	(1.1 ± 0.3) × 10 ⁻⁴⁹			0.0263		17
⁷⁶ Os ¹⁸⁸	633 ± 6	(2.0 ± 0.6) × 10 ⁻⁴⁹	2' → 0	(4.0 ± 1.2) × 10 ⁻⁵⁰	0.67 ± 0.10 ^c	15 ± 7 ^d	0.0132	$(8-4^{+20}) \times 10^{-5}$	6.3
	187	(2.53 ± 0.25) × 10 ⁻⁴⁸	2 → 0	(5.1 ± 0.5) × 10 ⁻⁴⁹			0.425		79
	370 ± 4		2' → 2	(2.1 ± 0.4) × 10 ⁻⁴⁹			0.051		32
	557 ± 6	(1.8 ± 0.4) × 10 ⁻⁴⁹	2' → 0	(3.6 ± 0.8) × 10 ⁻⁵⁰			0.0179		5.5
^{Os} 190	206	(2.04 ± 0.21) × 10 ⁻⁴⁸	2 → 0	(4.1 ± 0.4) × 10 ⁻⁴⁹	0.80 ± 0.15 ^e	-7 ^f	0.308	4×10^{-4}	62
	283 ± 3		2' → 2	(4.0 ± 1.0) × 10 ⁻⁴⁹			0.111		61
	489 ± 5	(2.1 ± 0.4) × 10 ⁻⁴⁹	2' → 0	(4.2 ± 0.8) × 10 ⁻⁵⁰			0.0246		6.4
	330	(1.94 ± 0.20) × 10 ⁻⁴⁸	2 → 0	(3.89 ± 0.39) × 10 ⁻⁴⁹			0.074		58
⁷⁸ Pt ¹⁹⁴	292		2' → 2	(2.3 ± 0.5) × 10 ⁻⁴⁹	3.3 ± 0.5 ^g	29 ± 26 ^h	0.107	10^{-3} to 10^{-5}	34
	622	(8.7 ± 2.0) × 10 ⁻⁵¹	2' → 0	(1.7 ± 0.4) × 10 ⁻⁵¹			0.016		0.25
	358	(1.27 ± 0.13) × 10 ⁻⁴⁸	2 → 0	(2.53 ± 0.25) × 10 ⁻⁴⁹			0.0598		37
	330		2' → 2				0.074		
Pt ¹⁹⁶	688	< 1.3 × 10 ⁻⁵¹	2' → 0	< 2.6 × 10 ⁻⁵²	> 2500 ⁱ	-4.36 ^j	0.0117		< 4 × 10 ⁻²

^a C. J. Gallagher, D. Strominger, and J. P. Unik, Phys. Rev. **110**, 725 (1958).^b E. Bodenstedt, E. Mathias, H. J. Korner, E. Gerdan, F. Frisius, and D. Hovestadt, Nuclear Phys. **15**, 239 (1960).^c M. W. Johns, C. C. McMullen, I. R. Williams, and V. S. Nablo, Can. J. Phys. **34**, 69 (1956).^d V. R. Potnis, V. S. Dubey, and C. E. Mandeville, Phys. Rev. **102**, 459 (1956).^e W. R. Kane, Harvard University, Department of Physics Technical Report No. 3-9, 1959 (unpublished); W. R. Kane, G. T. Emery, G. Scharff-Goldhaber, and M. McKeown, Phys. Rev. **119**, 1953 (1960).^f F. Cappellani, U. Farinelli, F. Ferrero, and R. Malvano, Physica **24**, 765 (1958).^g M. W. Johns and S. V. Nablo, Phys. Rev. **96**, 1599 (1954).^h C. E. Mandeville, J. Varma, and B. Saraf, Phys. Rev. **98**, 94 (1955).ⁱ D. E. Alburger, Phys. Rev. **108**, 812 (1957).^j R. M. Steffen, Phys. Rev. **89**, 665 (1953).

be expected. The coherent interference of the two modes of excitation can, under some circumstances, lead to appreciable errors in $B(E2)$. This problem has previously been discussed in connection with the α -particle Coulomb excitation of the second 2+ states of medium weight nuclei.¹¹ Since protons were used as projectiles in the present experiments, the importance of the "double $E2$ " interference is reduced. For the case in which "double $E2$ " excitation competes most favorably with direct $E2$, viz. 5-Mev protons on Pt¹⁹⁴, the "double $E2$ " cross section is still less than 1% of the direct $E2$ cross section. We have, however, included an error to take into account the possible uncertainty in $B(E2)_{\text{exo}}$ from this interference effect.

For several of the nuclei, the $B(E2)_{\text{exo}}$ for the second 2+ state was determined only from a coincident measurement. We have neglected the effect of the angular correlation of the cascade gamma rays from the sequence

$$0(E2)2(E2+M1)2(E2)0.$$

It is not practical to calculate the expected triple correlation for the geometry used in most of the measurements. In the case of Os¹⁹⁰ and Os¹⁹², we did measure the yields from a coincident spectrum in which the lower cascade gamma ray and the upper cascade gamma ray were observed at 0° and 90° with respect to the incident ion beam, respectively. The yields from these two geometric conditions agreed within 10%. For the latter geometry it is feasible to calculate the expected triple correlation by use of the Chalk River

tabulations.¹² Taking the upper cascade gamma ray as $E2$, the coincidence yield for Os¹⁹⁰ is 4% too large from the angular correlation effect at $E_p=5$ Mev. Although the yields in Table I do not include a correction for the angular correlation effect, we have assigned an error from this source of uncertainty to the $B(E2)_{\text{exo}}$ for the second 2+ state.

The total internal conversion coefficient α_T must be known in order to relate the cross sections to the observed gamma-ray yields. For this purpose the calculations of Rose and of Sliv and Band have been used.¹³ For the K and L shells, these calculations include the effect of the finite size of the nucleus. In the case of the M shell, the unscreened calculations by Rose have been used together with an empirical screening factor ($M_{\text{se}}/M_{\text{unse}}$)=0.6. For the N and O shells we have used $(N+O)/L=0.06$. The α_T 's are given in Table II.

To avoid confusion the reduced transition probabilities for excitation and for decay are written as $B(E2)_{\text{exo}}$ and $B(E2)_d$. In Table II we have taken $B(E2)_{\text{sp}}$ to be equal to $(1/4\pi)|\frac{3}{5}R|^2$ where $R=1.2 \times 10^{-13}A^{\frac{1}{3}}$ cm.¹⁴ For the purpose of discussing the results

¹² W. T. Sharp, J. M. Kennedy, B. J. Sears, and M. G. Hoyle, Chalk River Report CRT-556 (unpublished); J. M. Kennedy, B. J. Sears, and W. T. Sharp, Chalk River Report CRT-569 (unpublished); A. J. Ferguson and A. R. Rutledge, Chalk River Report CRT-615 (unpublished).

¹³ See, e.g., M. E. Rose, *Internal Conversion Coefficients* (North-Holland Publishing Company, Amsterdam, 1958), or L. A. Sliv and I. M. Band, Leningrad Physico-Technical Institute Reports, Part I, 1956; Part II, 1958 [translation: Reports 57ICC K1 and 58ICC L1, issued by Physics Department, University of Illinois, Urbana, Illinois (unpublished)].

¹⁴ J. M. Blatt and V. F. Weisskopf, *Theoretical Nuclear Physics* (John Wiley & Sons, Inc., New York, 1952), Chap. XII.

¹¹ P. H. Stelson and F. K. McGowan, Phys. Rev. **121**, 209 (1961).

TABLE III. Vibrational parameters for γ vibrations in even-even nuclei. The parameters $\hbar^2/2\mathcal{J}_0$ and F , which determine the level positions in the ground state rotational band, are also included: $E = (\hbar^2/2\mathcal{J}_0)I(I+1) - FI^2(I+1)^2$. These were obtained using only the $2+$ and $4+$ states.

Nucleus	$\hbar^2/2\mathcal{J}_0$ (kev)	β_0	C_γ (Mev)	\hbar^2/B_γ (Mev)	E_{2+} (kev)	E_{4+} (kev)	F (kev)
W ¹⁸⁴	18.65	0.244	20.1	0.036	111.1±0.06	363.9±0.1	$(2.29 \pm 0.10) \times 10^{-2}$
W ¹⁸⁶	20.47	0.222	13.4	0.035	122.5±0.1	406 ±3	$(0.8_{-0.4}^{+1.2}) \times 10^{-2}$
Os ¹⁸⁸	26.63	0.191	7.7	0.044	155.0±0.1	479 ±1	$(13.5 \pm 0.4) \times 10^{-2}$
Os ¹⁹⁰ ^a	32.82	0.167	5.7	0.042	186.7±0.1	547.7±0.5	$(26.6 \pm 0.4) \times 10^{-2}$

^a The levels of the ground state rotational band of Os¹⁹⁰ are not fitted by the addition of the correction term arising from the rotation-vibration interaction (see reference 20).

we have included the $B(E2)_{\text{ex}}$ for the first $2+$ state in Table II.

III. DISCUSSION OF REDUCED TRANSITION PROBABILITIES

The lowest excitations of W¹⁸⁴ and W¹⁸⁶ correspond to a rotational spectrum of permanently deformed nuclei (see Fig. 4). As previously mentioned, one may also expect these nuclei to exhibit collective excitations which correspond to vibrations about the equilibrium shape. According to the collective model,¹⁵ the $2+\beta$ -vibrational excitation decays by means of $E2$ radiation to the $I=0+$, $2+$, and $4+$ members of the ground-state band with relative reduced transition probabilities 7:10:18. For the $2+$ γ -vibrational excitation, the corresponding relative reduced transition probabilities are 7:10:1/2. From the Coulomb excitation measurements of the second $2+$ states in W¹⁸⁴ and W¹⁸⁶, it is not possible to draw conclusions concerning the type of the vibrational excitation. For instance, in the case of W¹⁸⁶, the intensity of the $2' \rightarrow 4$ transition should be 4.5% and 0.12% of the ground state transition ($2' \rightarrow 0$) for β - and γ -vibrational excitations, respectively. In either case the intensity of the $2' \rightarrow 4$ transition is too weak to detect in our measurements. We have therefore relied on information from radioactive decay studies to characterize the type of vibrational excitation in W¹⁸⁴ and W¹⁸⁶.

Several groups¹⁶⁻¹⁸ of workers have studied the decay of Re¹⁸⁴ \rightarrow W¹⁸⁴. Gallagher *et al.* and Johnson obtained values of 0.088 and 0.25 for the ratio $B(E2, 2' \rightarrow 4)/B(E2, 2' \rightarrow 0)$. These values favor the assignment of a $2+$ γ -vibrational state at 891 kev in W¹⁸⁴.^{18a} Confirmation of this assignment is obtained from gamma-gamma angular correlation measurements by Bodensedt *et al.* The angular distribution of the gamma-ray cascade from the decay of a state at 1006 kev is consistent with a decay sequence $3(E2)2(E2)0$. The $3+$ state is

¹⁵ K. Alder, A. Bohr, T. Huus, B. R. Mottelson, and A. Winther, *Revs. Modern Phys.* **28**, 432 (1956).

¹⁶ C. J. Gallagher, D. Strominger, and J. P. Unik, *Phys. Rev.* **110**, 725 (1958).

¹⁷ Noah Johnson (private communication, 1958).

¹⁸ E. Bodensedt, E. Mathias, H. J. Korner, E. Gerdan, F. Frisius, and D. Hovestadt, *Nuclear Phys.* **15**, 239 (1960).

^{18a} Note added in proof. We interpret the state at 891 kev to correspond to the 904-kev state observed in the radioactive decay measurements.

interpreted as a rotational state associated with the γ -vibrational excitation. The moment of inertia of this rotational band is nearly equal (within a few percent) to that of the ground state rotational band.

From the knowledge of both the position and the $B(E2)_{\text{ex}}$ for a vibrational state, one can deduce the vibrational parameters B_2 and C_2 , where B_2 is the mass transport associated with the vibrational motion and C_2 represents the effective surface tension. For the γ -vibrational excitation we use¹⁹

$$\hbar\omega_\gamma = \hbar(C_\gamma/B_\gamma)^{1/2},$$

$$B(E2, 0 \rightarrow 2(\gamma)) = \left(\frac{3}{4\pi} ZeR^2\right)^2 \beta_0^2 \frac{\hbar}{(B_\gamma C_\gamma)^{1/2}},$$

where $\hbar\omega_\gamma = E_{2(\gamma)} - \hbar^2/\mathcal{J}$. The moment of inertia \mathcal{J} is taken equal to \mathcal{J}_0 , the moment inertia associated with the ground-state band. β_0 is deduced from the $B(E2, 0 \rightarrow 2)$ to the first rotational level of the ground-state band. The vibrational parameters for W¹⁸⁴, W¹⁸⁶, Os¹⁸⁸, and Os¹⁹⁰ are given in Table III. Scharff-Goldhaber *et al.*²⁰ have observed gamma rays following the decay of a high-lying isomer in Os¹⁹⁰, and this decay excites a rotational spin sequence. There is, however, considerable departure from the $I(I+1)$ law for the level position in a rotational band.

The interaction between the rotational and the vibrational motion gives rise to two corrections to the rotational level spacing of the ground state band. The nucleus deviates from axial symmetry during γ vibrations and the moment of inertia \mathcal{J}_0 changes during β vibrations. The corrections to the energy of the rota-

TABLE IV. Vibrational parameters C_2 and B_2 for quadrupole vibrations about the spherical shape and the parameter β for the "shape unstable" model of the nucleus.

Nucleus	C_2 (Mev)	$B_2/(B_2)_{\text{irrot}}$	β
Os ¹⁹²	19.1	17.0	0.171
Pt ¹⁹⁴	34.4	11.8	0.155
Pt ¹⁹⁶	58.6	16.7	0.125

¹⁹ B. L. Birbrair, L. K. Peker, and L. A. Sliv, *J. Exptl. Theoret. Phys. (U.S.S.R.)* **36**, 803 (1959) [translation: *Soviet Physics—JETP* **9**, 566 (1959)].

²⁰ G. Scharff-Goldhaber, D. E. Alburger, G. Harbottle, and M. McKeown, *Phys. Rev.* **111**, 913 (1958).

TABLE V. Comparison with Davydov-Filippov model. γ is deduced from the positions of the first and second 2+ states.

Nucleus	γ (deg)	$B(E2, 2' \rightarrow 2)/B(E2, 2 \rightarrow 0)$		$B(E2, 2' \rightarrow 0)/B(E2, 2 \rightarrow 0)$		$B(E2, 2' \rightarrow 2)/B(E2, 2' \rightarrow 0)$	
		Theory	Exp	Theory	Exp	Theory	Exp
W ¹⁸⁴	13.9	0.12	0.07±0.02	0.051	0.038±0.012	2.40	1.9± 0.4
W ¹⁸⁶	16.0	0.18	0.12±0.02	0.061	0.048±0.010	3.05	2.5± 0.5
Os ¹⁸⁸	19.1	0.32	0.19±0.06	0.071	0.070±0.022	4.60	2.8± 0.4
Os ¹⁹⁰	22.3	0.58	0.41±0.09	0.067	0.071±0.017	8.7	5.8± 1.1
Os ¹⁹²	25.3	0.94	0.98±0.26	0.042	0.102±0.023	23.5	9.5± 2.4
Pt ¹⁹⁴	0.59±0.14	...	0.004±0.001	...	135 ±20

tional levels in the ground state band are given by¹⁹

$$\Delta E_\gamma = -\frac{1}{6C_\gamma} \left(\frac{\hbar^2}{\mathcal{J}_0} \right)^2 I^2(I+1)^2,$$

$$\Delta E_\beta = -\frac{1}{2C_\beta} \left(\frac{\partial}{\partial \beta} \frac{\hbar^2}{2\mathcal{J}_0} \right)^2 I^2(I+1)^2.$$

In Table III we have also included the parameters $\hbar^2/2\mathcal{J}_0$ and F deduced from the known level positions (for $I=2$ and 4) of the ground-state band. The parameter F is related to ΔE_γ and ΔE_β by

$$\Delta E_\gamma + \Delta E_\beta = -FI^2(I+1)^2.$$

On inserting the values of C_γ in Table III into ΔE_γ , we find that $(1/6C_\gamma)(\hbar^2/\mathcal{J}_0)^2$ is about 50% of F given in Table III. No estimate of the contribution from ΔE_β to F can be made because there is no information available for

$$C_\beta \text{ and } \frac{\partial}{\partial \beta} \left(\frac{\hbar^2}{2\mathcal{J}_0} \right).$$

For irrotational collective flow²¹ the moment of inertia is related to the mass parameter B_γ by

$$\hbar^2/B_\gamma = 3\hbar^2/\mathcal{J}_{\text{irrot.}}$$

Some calculations of Tamura and Udagawa²² suggest that this relation may also be approximately true without making the assumption of irrotational flow. However, inserting the experimental values obtained for \mathcal{J}_0 and B_γ , we find that

$$(3\hbar^2/\mathcal{J}_0)/(\hbar^2/B_\gamma) \approx 3.5;$$

a value considerably different from the expected value of 1.

A striking feature of the 2+ γ -vibrational excitation is the rapid decrease in energy of this state with the decrease in the equilibrium deformation β_0 (see Fig. 4 and Table III). In this transition region of decreasing deformation, the ratio $E_{2(\gamma)}/\beta_0$ is remarkably constant (3.47 ± 0.18 Mev) for W¹⁸⁴, W¹⁸⁶, Os¹⁸⁸, and Os¹⁹⁰. The same may be true for the region near thorium ($E_{2(\gamma)}/\beta_0 = 3.26$ Mev for Th²³²).

²¹ A. Bohr, Kgl. Danske Videnskab. Selskab, Mat.-fys. Medd. 26, No. 14 (1952).

²² T. Tamura and T. Udagawa, Nuclear Phys. 16, 460 (1960).

The spectrum of the low-lying levels of the other nuclei (Os¹⁹², Pt¹⁹⁴, and Pt¹⁹⁶) suggests a possible interpretation as "near harmonic" motion of spherical nuclei. In this case the vibrational parameters B_2 and C_2 for quadrupole vibrations about the spherical shape are obtained from the $B(E2)_{\text{exc}}$ and the E_{2+} for the first 2+ state.¹⁵ The values for C_2 and $B_2/(B_2)_{\text{irrot}}$ are listed in Table IV.

The "shape unstable" model²³ has also been proposed to account for the "near harmonic" spectra. The parameters appropriate to this model are β and $B_2/(B_2)_{\text{irrot}}$. The values for β are listed in Table IV. The values of the parameters are similar to those observed for medium weight even-even nuclei.⁷

The $B(E2)$ values for the crossover transition from the second 2+ state to the ground state exhibit some uniformity for the even-even nuclei of tungsten and osmium, being about 6 times $B(E2)_{\text{sp.}}$. This is in qualitative agreement with the prediction of the collective model for vibrations of spheroidal nuclei.

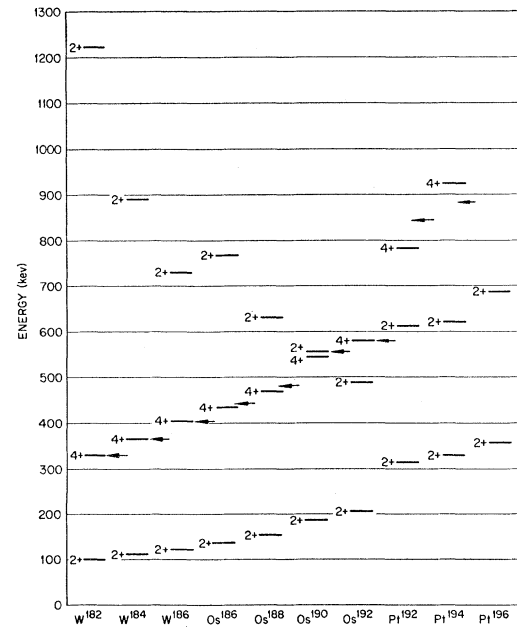


FIG. 4. Low-lying levels for even-even nuclei in the transition region from spheroidal to spherical shape.

²³ L. Wilets and M. Jean, Phys. Rev. 102, 788 (1956).

The $B(M1)$ values for the $2' \rightarrow 2$ transition are exceedingly small compared to the single-particle estimate. These small values are in qualitative agreement with the collective models, i.e., $M1$ radiation is forbidden in the decay of vibrational excitations.

In Table V the ratios of $B(E2)$ are compared with the predictions of the various collective models. The strong coupling model for axial symmetric nuclei predicts that $B(E2, 2' \rightarrow 2)/B(E2, 2' \rightarrow 0)$ is 1.43. The observed values for W^{184} and W^{186} are appreciably larger. The models for vibrations of spherical nuclei and "shape unstable" nuclei predict (in the simplest approximation) that $B(E2, 2' \rightarrow 2)/B(E2, 2 \rightarrow 0)$ should be 2. The observed values for Pt^{194} and Os^{192} are somewhat less than 2.

The predictions of the asymmetric rotor model of Davydov and Filippov⁴ are particularly interesting since this model offers a possible quantitative interpretation of collective motion in a transition region such as that represented by the osmium nuclei. The positions

of the first and second $2+$ states and the first $4+$ state are shown in Fig. 4 for the even- A nuclei of wolfram, osmium, and platinum. According to the Davydov-Filippov model the parameter γ , which measures the departure from axial symmetry, can be obtained from the ratio of the energies of the first and second $2+$ states. When one has the value for γ and the energy of the first $2+$ state, one can then predict the expected positions of the first $4+$ state. The expected locations of the $4+$ state are indicated by arrows in Fig. 4. There is rather good agreement between the predicted locations and the observed locations of the first $4+$ state.

The Davydov-Filippov model also makes quantitative predictions for the ratios of $B(E2)$ for these nuclei. In Table V we have compared our results with the predictions of this model. The model predicts quite well the observed trends in the ratios of the $B(E2)$'s and, in fact, there is considerable quantitative agreement.

Fast Neutron Activation Cross Section of Au^{197} †

S. A. Cox

Argonne National Laboratory, Argonne, Illinois

(Received November 3, 1960)

The neutron activation cross section of gold was measured in the neutron range from 30–1500 kev. The absolute value of the cross section was based on the U^{235} fast fission cross section which was used for absolute neutron flux measurements from 200–1500 kev. For measurements below 200 kev, the $B^{10}(n, \alpha)$ cross section was used for monitoring the neutron flux. The relative cross section from 30–200 kev was then normalized at 200 kev to the absolute measurement. The results agree well with recent measurements, except for some pulsed beam—liquid scintillator measurements and spherical shell transmission measurements which yield much lower cross section values.

INTRODUCTION

A KNOWLEDGE of the absolute value and energy dependence of neutron capture cross sections is important to the design of nuclear reactors. Previously there has been considerable disagreement between measurements made by different groups in both the absolute value and energy dependence of capture cross sections. To a large degree, the disagreement in the absolute value of the capture cross section has been removed in the region of incident neutron energy above approximately 200 kev. However, disagreement in the shape and absolute value of the cross section below 200 kev still exists. This measurement is presented to give additional information on both points for the gold activation cross section.

† Work performed under the auspices of the U. S. Atomic Energy Commission.

EXPERIMENTAL PROCEDURE

The analyzed proton beam from the Argonne 3-Mev Van de Graaff accelerator was used to produce neutrons from the $Li^7(p, n)Be^7$ reaction. The lithium films were evaporated in vacuum onto tantalum target cups. For gold irradiations in the neutron energy range from 20–200 kev, the lithium targets were 10–20 kev thick to the incident protons. For irradiations with neutron energies above 200 kev, the lithium targets were approximately 50 kev thick to the incident protons. The gold was irradiated for approximately one-half hour and then was immediately transferred to a shielded NaI(Tl) scintillation spectrometer where the gamma ray activity was measured. All gold samples were counted within a few minutes after irradiation. The activation cross section was calculated from the known integrated neutron flux, the known gamma-ray efficiency of the scintillation